

## Investigation on correlation between pulse velocity and compressive strength of concrete using ANNs

Chao-Wei Tang<sup>†</sup>

*Department of Civil Engineering & Engineering Informatics,  
Cheng-Shiu University, Taiwan, R.O.C.*

Yiching Lin<sup>\*</sup> and Shih-Fang Kuo<sup>‡†</sup>

*Department of Civil Engineering, National Chung Hsing University, Taiwan, R.O.C.  
(Received June 7, 2007, Accepted November 30, 2007)*

**Abstract** The ultrasonic pulse velocity method has been widely used to evaluate the quality of concrete and assess the structural integrity of concrete structures. But its use for predicting strength is still limited since there are many variables affecting the relationship between strength and pulse velocity of concrete. This study is focused on establishing a complicated correlation between known input data, such as pulse velocity and mixture proportions of concrete, and a certain output (compressive strength of concrete) using artificial neural networks (ANN). In addition, the results predicted by the developed multilayer perceptrons (MLP) networks are compared with those by conventional regression analysis. The result shows that the correlation between pulse velocity and compressive strength of concrete at various ages can be well established by using ANN and the accuracy of the estimates depends on the quality of the information used to train the network. Moreover, compared with the conventional approach, the proposed method gives a better prediction, both in terms of coefficients of determination and root-mean-square error.

**Keywords:** ultrasonic pulse velocity; concrete compressive strength; artificial neural network; multilayer perceptrons.

---

### 1. Introduction

In engineering practice, compressive strength is the most important index to assess the quality of concrete. This is because many properties of concrete, such as elastic modulus, water tightness or impermeability, and resistance to weathering agents, are directly or indirectly related to strength and thus can be deduced from the strength data. In view of this, various nondestructive testing (NDT) methods have been developed to predict concrete compressive strength over the last decades. Among them, the ultrasonic pulse velocity (UPV) method that has been used widely in laboratory as well as in the field appears to be the most popular one.

The UPV method is based on physical laws of elastic stress wave propagation in solids.

---

<sup>†</sup> Associate Professor, Corresponding Author, E-mail: [tangcw@csu.edu.tw](mailto:tangcw@csu.edu.tw)

<sup>‡</sup> Professor

<sup>‡†</sup> Ph.D.

Generally speaking, the advantages of the UPV method include easy operation and high repeatability. Accordingly, it has served as an important NDT technique for concrete quality control and quality assurance, as well as for deterioration evaluation of concrete. However, it should be noted that the pulse velocity are influenced by many factors in concrete, but those factors might have little influences on concrete strength (Sturup, *et al.* 1984, Yun, *et al.* 1988, Kheder 1998, Shikh 1998). To establish the relationships between strength and pulse velocity of concrete, a number of experimental studies have been conducted since the 1950s (Andersen and Nerenst 1952, Galan 1967, Chung and Law 1983, Popovics, *et al.* 1990, Phoon, *et al.* 1999, Liang and Wu 2002, Lin, *et al.* 2003, Kewalramani and Gupta 2006). And the results show that a relationship with a wide variation will be acquired if the data of pulse velocity,  $v$ , and the compressive strength,  $f'_c$ , of concrete having different mixture proportions are pooled together to analyze. However, a strength estimate made with the pulse velocity method is reliable if a pre-established calibration curve is available (Jones and Gatfield 1955, Demirboga, *et al.* 2004).

Essentially, the compressive strength of concrete can be expressed as a nonlinear function of mixture proportions, aggregate type, age of concrete, moisture content, pulse velocity, and others. Theoretically, a multivariable nonlinear regression analysis can be performed to derive relationships among the parameters involved, but it is practically difficult to apply the statistical approach in a complex nonlinear system. By contrast, artificial neural networks (ANN) are a family of massively parallel architectures that solve difficult problems via the cooperation of highly interconnected but simple artificial neurons (Zurada 1992, Fausset 1994). Therefore, the approach is particularly attractive for those problems where the solution algorithm is unknown or too complicated to solve the problems directly. In fact, the methodology of ANN has been successfully applied in civil engineering to model the structural behavior and properties of concrete materials such as strength, durability, expansion, and constitutive modeling (Ghaboussi, *et al.* 1991, Tang, *et al.* 2003, Yeh 1999, Zhao and Ren 2002, Tang 2006, Hossain, *et al.* 2006).

Currently, the use of pulse velocity for evaluation of concrete strength was constrained by the fact that a correlation between pulse velocity and compressive strength must be pre-established for a particular concrete. The ANN computational tool is needed to break the constraint. The present study uses UPV and mixture proportions of concrete specimen as predictive variables for prediction of compressive strength of concrete at various ages. The specimen compositions vary widely in aggregate content and water-cement ratio. Then different models including neural networks and regression analysis for investigation on pulse velocity-strength relationship of concrete are discussed. In addition, a comparative study between the neural network and regression analysis models is also carried out. The results of the studies can help improve the application of pulse velocity to evaluation of concrete strength.

## 2. Artificial neural network

### 2.1. Architecture of MLP networks

The most commonly used ANN is probably the multilayer perceptrons (MLP) network. Fig. 1 shows a typical MLP network trained by back-propagation algorithm. It consists of an input layer, an output layer, and one hidden layer, where  $X_1, X_2, \dots, X_N$  are the  $N$  components of input vector  $X$ ,

$W_{ji}$  and  $W_{kj}$  are the connection weights between neurons of different layers,  $\theta_j$  is the bias assigned to neuron  $j$  in the hidden layer, and  $\theta_k$  is the bias assigned to neuron  $k$  in the output layer. Neurons in the input layer represent the possible influential factors that affect the network outputs, while the output layer contains one or more neurons that produce the network outputs. Layers between the input and output layers are called hidden layers and contain a large number of hidden neurons.

Fig. 2 shows a typical neuron selected from hidden or output layers of a neural network. Each neuron forms a weighted sum

$$\sum_{i=1}^N W_{ji} X_i \tag{1}$$

of  $N$  inputs from previous layer, and a bias is  $\theta_j$  added.

$$U_j = \sum_{i=1}^N W_{ji} X_i + \theta_j \tag{2}$$

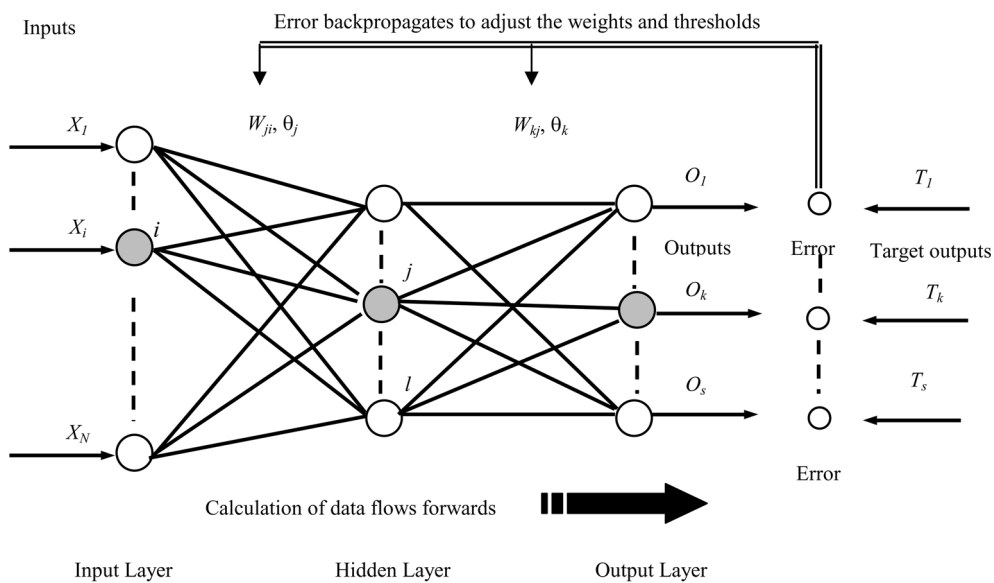


Fig. 1 Architecture of a typical MLP network trained by back-propagation algorithm

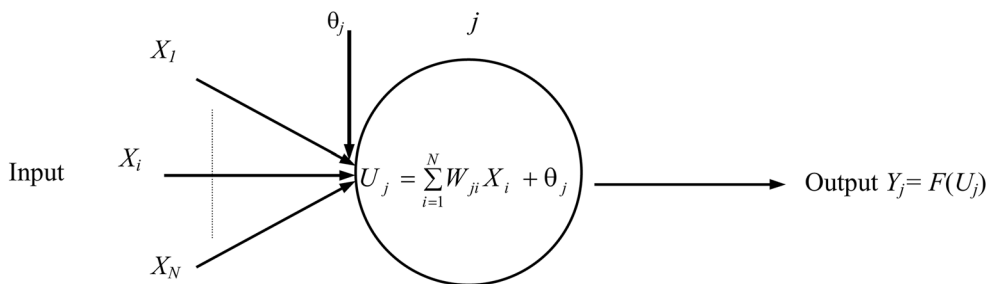


Fig. 2 A typical neuron selected from hidden or output layers of a neural network

where  $W_{ji}$  is termed the weighted coefficient, and the subscript  $ji$  denotes that  $W_{ji}$  is the connection weight on the link from neuron  $i$  in the previous layer to neuron  $j$  in the current layer. Then the sum becomes the input signal of the processing unit. Processing units process and pass the results through an activation function  $F$  to obtain its output  $Y_j$  as follows:

$$Y_j = F(U_j) = F\left(\sum_{i=1}^N W_{ji}X_i + \theta_j\right) \quad (3)$$

As the name of back-propagation algorithm indicates, propagation takes place in a feed-forward manner from the input layer to the output layer when a set of input patterns is presented to the network, and backward error propagation begins at the output layer using a learning mechanism to adjust the weights and biases when errors propagate through the intermediate layers toward the input layer. Taking the  $k$ th neuron in the output layer as an example (Fig. 1), the error  $E$  between the calculated value  $O_k$  and the desired value  $T_k$  of output layer neurons may be defined as

$$E = \frac{1}{2} \sum_{k=1}^s (O_k - T_k)^2 \quad (4)$$

where

$$O_k = F(U_k) = F\left(\sum_{j=1}^l W_{kj}Y_j + \theta_k\right) \quad (5)$$

## 2.2. Training algorithm of MLP networks

The learning mechanism of MLP networks with back-propagation algorithm is a generalized delta rule that uses the gradient-descent method to minimize the error between the actual and the desired output (Rumelhart, *et al.* 1986). From hidden to output, the modification of weights and biases are represented respectively by the following expressions:

$$\Delta W_{kj} = \eta \delta_k Y_j \quad (6)$$

$$\Delta \theta_k = \eta \delta_k \quad (7)$$

where

$\eta$  = learning rate

$$\delta_k = (T_k - O_k) F'(U_k)$$

And from input to hidden

$$\Delta W_{ji} = \eta \delta_j X_i \quad (8)$$

$$\Delta \theta_j = \eta \delta_j \quad (9)$$

where

$$\delta_j = \sum_k W_{kj} \delta_k F'(U_j)$$

The training algorithm may be improved by adding momentum terms into Eq. (6) to Eq. (9). The process of forward and backward propagation continues until the error is reduced to an acceptable level.

### **3. Experimental details**

#### *3.1. Materials*

The test program started with materials selections. The selected ingredients included Type I Portland cement, coarse aggregate with a maximum size of 12.7 mm, fine aggregate with a fineness modulus of 3.12, and superplasticizer. The superplasticizer used is a special high molecular superplasticized retardant conforming to ASTM C-494 Type *F*.

#### *3.2. Mixture proportions and fabrication of specimens*

The experimental work consists of two parts. Part 1 contains fifteen concrete mixture proportions identified as N1 to N15 that were used to train the established ANN models. Details of the mixture proportions are provided in Table 1. The water-cement ratio (W/C) ranges from 0.3 to 0.7. For all the fifteen mixture proportions, the cement paste occupies 36% of the total concrete volume. Three volume ratios of fine aggregate to total aggregate (S/A: Sand/Aggregate) are considered to be 30%, 45%, and 60% for each water-cement ratio. After mixing, fifteen specimens were produced for each mixture proportion. All the specimens were cast in 100×200 mm cylindrical steel molds and kept in their molds for about 24 hours in the laboratory and then de-molded. Three concrete cylinders were tested at an age of 1 day and all other concrete cylinders were cured in water at 20°C and tested at ages of 3, 7, 14, and 28 days, respectively. At each age, the pulse velocity and compressive strength of three specimens were measured according to the specification of ASTM C597 (1998) and ASTM C39 (1998), respectively.

Part 2 contains nine concrete mixture proportions identified as N16 to N24 that were used to test the validity of the established MLP network models. Details are provided in Table 2. Three specimens were produced for each mixture proportion. A total of 108 concrete specimens were prepared for tests at ages of 3, 7, 14, and 28 days, respectively.

#### *3.3. Instrumentation and test procedures*

Through a direct transmission (pitch-catch) mode as illustrated in Fig. 3, ultrasonic pulse velocities were measured by a commercially available pulse meter with an associated transducer pair. The principle of ultrasonic pulse velocity measurement involves sending an electro-acoustic pulse into concrete and measuring the travel time for the pulse to propagate through the concrete. The pulse is generated by a transmitter and received by a receiver. Knowing the path length, the measured travel time ( $\Delta t$ ) can be used to calculate the pulse velocity ( $v$ ) as follows:

$$v = D/\Delta t \quad (10)$$

where  $D$  is the depth of the cylinder. The concrete surface must be prepared in advance for a proper acoustic coupling. A small pressure is needed to ensure firm contact of the transducers against the concrete surface. On the other hand, compression testing of cylindrical specimens was performed using a servo-hydraulic material testing system.

Table 1 Experimental data for training and verification sets

Mix No.	$W/C^1$	$S/A^2$ (%)	Mixture proportion (kg/m <sup>3</sup> )					Age (Day)	Test Results		Type of subset
			Cement	Water	$FA^3$	$CA^4$	$SP^5$		$v^6$ (m/sec)	$f_c^7$ (MPa)	
N1	30				501	1165		1	3315	3.7	training
								3	3705	7.0	training
								7	4010	11.4	training
								14	4084	14.1	verification
								28	4134	16.2	training
N2	0.7	45	354	248	752	915	0.00	1	3396	5.3	training
								3	3772	10.1	training
								7	4001	13.7	training
								14	4104	18.5	verification
								28	4164	21.5	training
N3	60				1002	666		1	3382	7.0	training
								3	3771	14.1	verification
								7	4037	20.8	training
								14	4084	25.8	training
								28	4141	29.3	training
N4	30				501	1165		1	3441	6.2	verification
								3	3888	12.9	training
								7	4155	18.5	verification
								14	4240	22.0	training
								28	4300	24.5	training
N5	0.6	45	392	235	752	915	0.98	1	3538	8.2	training
								3	3847	17.1	verification
								7	4158	22.7	verification
								14	4219	27.9	verification
								28	4245	29.7	training
N6	60				1002	666		1	3577	9.4	training
								3	3855	18.0	verification
								7	4142	25.2	training
								14	4213	27.3	training
								28	4279	34.7	training
N7	30				501	1165		1	3794	12.0	verification
								3	4093	23.3	training
								7	4336	27.9	training
								14	4376	34.0	training
								28	4450	36.1	training
N8	0.5	45	440	219	752	915	2.20	1	3803	14.0	training
								3	4133	27.5	training
								7	4295	37.0	training
								14	4388	42.8	verification
								28	4451	45.6	training
N9	60				1002	666		1	3719	13.1	training
								3	4033	25.2	training
								7	4221	34.2	training
								14	4291	41.1	verification
								28	4369	46.1	training

Table 1 Experimental data for training and verification sets (Continued)

Mix No.	$W/C^1$	$S/A^2$ (%)	Mixture proportion (kg/m <sup>3</sup> )					Age (Day)	Test Results		Type of subset
			Cement	Water	$FA^3$	$CA^4$	$SP^5$		$v^6$ (m/sec)	$f_c^7$ (MPa)	
N10	30				501	1165		1	4050	23.4	training
								3	4307	34.3	verification
								7	4467	42.6	verification
								14	4517	48.6	verification
								28	4593	53.6	training
N11	0.4	45	500	197	752	915	4.99	1	4021	24.9	training
								3	4290	39.0	training
								7	4404	45.6	training
								14	4481	50.0	verification
								28	4563	53.7	verification
N12	60				1002	666		1	3984	24.6	training
								3	4240	41.6	training
								7	4322	44.9	verification
								14	4453	51.3	verification
								28	4498	55.5	verification
N13	30				501	1165		1	4303	38.5	verification
								3	4477	55.2	training
								7	4546	58.1	training
								14	4609	65.4	training
								28	4706	67.3	training
N14	0.3	45	578	169	752	915	8.68	1	4222	41.6	verification
								3	4452	56.1	training
								7	4513	62.3	training
								14	4593	65.4	training
								28	4612	71.0	verification
N15	60				1002	666		1	4260	45.0	verification
								3	4414	58.9	training
								7	4494	62.8	training
								14	4583	68.5	training
								28	4629	74.2	verification

Notes: <sup>1</sup> $W/C$ =Water-cement ratio; <sup>2</sup> $S/A$ =Volume ratio of fine aggregate to total aggregate; <sup>3</sup> $FA$ =Fine Aggregate; <sup>4</sup> $CA$ =Coarse Aggregate; <sup>5</sup> $SP$ =Superplasticizer; <sup>6</sup> $v$ =Ultrasonic pulse velocity; <sup>7</sup> $f_c$ =Compressive strength.

#### 4. Artificial neural network analysis

To investigate the correlation between pulse velocity and compressive strength development of concrete, a commercially available software package, STATISTICA Neural Networks (SNN), was used. Details on the establishment of neural network-based analysis models are described below.

Table 2 Experimental data for test set

Mix No.	W/C	S/A (%)	Mixture proportion (kg/m <sup>3</sup> )					Age (Day)	Test Results		Type of subset
			Cement	Water	FA	CA	SP		$\nu$ (m/sec)	$f'_c$ (MPa)	
N16	28				460	1175		3	3919	13.7	
								7	4190	18.8	
								14	4252	20.7	
								28	4340	22.6	
N17	36		354	248	592	1044	0.00	3	3896	13.7	
								7	4187	19.3	
								14	4268	23.8	
								28	4317	23.4	
N18	44				723	914		3	3924	15.5	
								7	4151	22.0	
								14	4223	25.9	
								28	4277	26.3	
N19	52				855	783		3	3994	17.2	
								7	4213	23.8	
								14	4299	27.2	
								28	4371	30.5	
N20	28				460	1175		3	4120	19.7	test
								7	4315	27.5	
								14	4393	30.8	
								28	4455	33.0	
N21	0.6	36	392	235	592	1044	0.98	3	4146	21.1	
								7	4342	28.9	
								14	4405	32.5	
								28	4454	34.9	
N22	44				723	914		3	4101	23.1	
								7	4291	31.7	
								14	4363	36.0	
								28	4407	38.2	
N23	0.5	52	441	218	855	783	2.20	3	4277	36.8	
								7	4400	45.2	
								14	4478	50.4	
								28	4550	51.1	
N24	0.4	52	502	196	855	783	5.02	3	4375	47.5	
								7	4470	50.8	
								14	4534	59.0	
								28	4600	59.2	

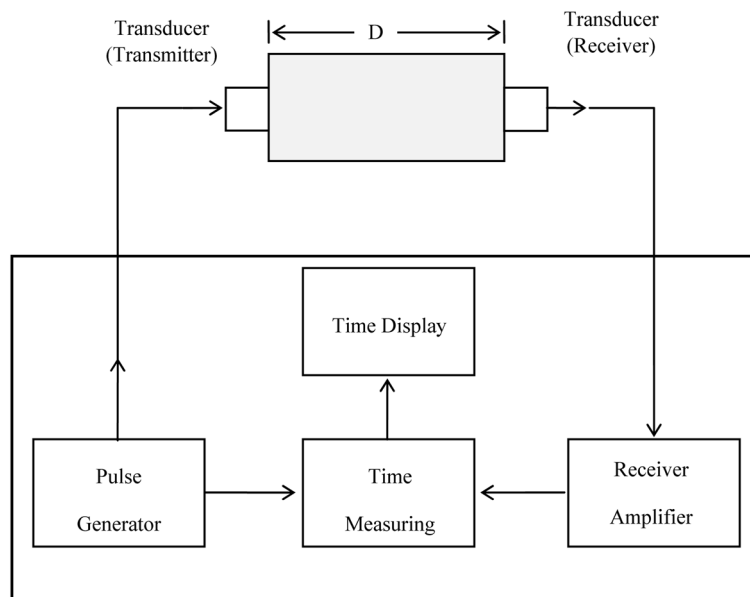


Fig. 3 Schematic diagram of pulse velocity testing circuit

#### 4.1. Data set

The measurement results of concrete pulse velocity along with corresponding compressive strength are listed in Table 1 and Table 2. Each value was the average of three concrete cylinders for each mixture proportion at a specific age. Seventy-five experimental data listed in Table 1 are used to train and verify the artificial neural network. Among them, 50 records are sampled randomly as training examples, and the remaining 25 records are regarded as verifying examples. On the other hand, thirty-six records given in Table 2 are used as testing examples to check the generalization of the model developed by the current studies.

#### 4.2. System model

Determining the network architecture is one of the most important tasks in the development of MLP network models. It requires the selection of the input and output parameters which will restrict the number of the input and output neurons of the network. In the study the compressive strength development of concrete  $f'_c$  is selected as the output variable. Because there are too many input variables, a sensitivity analysis was carried out first to determine the impact of each input on the neural network performance. In other words, all possible variables including ultrasonic pulse velocity  $v$ , dosage of cement  $C$ , dosage of water  $W$ , fine aggregate content  $FA$ , coarse aggregate content  $CA$ , dosage of superplasticizer  $SP$ , and testing age of the concrete cylinders  $T$  are considered in an initial development stage. In the study sensitivity provided by the SNN software package is reported separately for training and verification subsets, and the results show that the consistency of the sensitivity ratings between these two subsets is a good initial cross check on the reliability of the sensitivity analysis. For MLP network with 3 layers the sensitivity analysis shows the following sequence of importance of the variables:  $v$ ,  $CA$ ,  $FA$ ,  $W$ ,  $C$ ,  $SP$ , and  $T$ . It should be noted that the

Table 3 Architecture of ANN models

Model	Inputs variables	Output variable	Number of neurons			
			Input layer	1 <sup>st</sup> Hidden layer	2 <sup>nd</sup> Hidden layer	Output layer
M3:1-2-1	$v$	$f'_c$	1	2	-	1
M3:2-1-1	$v, W$	$f'_c$	2	1	-	1
M3:3-3-1	$v, CA, W$	$f'_c$	3	3	-	1
M3:4-3-1	$v, CA, W, SP$	$f'_c$	4	3	-	1
M3:5-3-1	$v, CA, W, FA, T$	$f'_c$	5	3	-	1
M3:6-5-1	$v, CA, W, FA, SP, C$	$f'_c$	6	5	-	1
M3:7-6-1	$v, CA, W, FA, SP, C, T$	$f'_c$	7	6	-	1
M4:1-5-5-1	$v$	$f'_c$	1	5	5	1
M4:2-2-2-1	$v, W$	$f'_c$	2	2	2	1
M4:3-5-1-1	$v, CA, W$	$f'_c$	3	5	1	1
M4:4-8-5-1	$v, CA, W, SP$	$f'_c$	4	8	5	1
M4:5-13-7-1	$v, CA, W, C, SP$	$f'_c$	5	13	7	1
M4:6-20-7-1	$v, CA, W, FA, SP, C$	$f'_c$	6	20	7	1
M4:7-11-10-1	$v, CA, W, FA, SP, C, T$	$f'_c$	7	11	10	1

Table 4 Sensitivity analysis of variables

ANN Model	Ranking of variable						
	$v$	$C$	$W$	$FA$	$CA$	$T$	$SP$
M3:1-2-1	1	-	-	-	-	-	-
M3:2-1-1	1	-	2	-	-	-	-
M3:3-3-1	1	-	2	-	3	-	-
M3:4-3-1	1	-	2	-	4	-	3
M3:5-3-1	1	-	3	4	2	5	-
M3:6-5-1	1	5	2	6	4	-	3
M3:7-6-1	1	5	4	3	2	7	6
M4:1-5-5-1	1	-	-	-	-	-	-
M4:2-2-2-1	1	-	2	-	-	-	-
M4:3-5-1-1	1	-	2	3	-	-	-
M4:4-8-5-1	1	-	2	4	3	-	-
M4:5-13-7-1	1	-	2	5	3	-	4
M4:6-20-7-1	1	6	2	4	3	-	5
M4:7-11-10-1	1	6	2	4	3	7	5

least influence on the prediction of  $f'_c$  is the variable  $T$  and this might be due to possible redundancy and interdependence between  $v$  and  $T$ .

Practically, a neural network with less input is usually preferable. Accordingly, several MLP network models, which use a few parameters as the input variables, were also developed. However, no specific guidelines exist on how to choose the number of hidden layer and neurons in the hidden layer. Therefore, the numbers of hidden layer and neuron are determined through a trial-and-error

process. After trials of different hidden layers and neurons, several models are considered for predicting the compressive strength of concrete. The architecture of the developed MLP network models is shown in Table 3. The first column in Table 3 denotes the neural network structure. For example, M3:3-3-1 stands for the network model using MLP network with 3 layers, 3 input neurons in the first layer, 1 hidden layer with 3 hidden neurons in the second layer, and 1 output neuron in the third layer. Table 4 shows the results obtained from the sensitivity analysis of the models proposed in Table 3. It reveals that the main variables having significant influence on the prediction of  $v$  include  $v$ ,  $CA$ ,  $W$ , and  $FA$ .

#### *4.3. Training algorithm*

First, to avoid the slow rate of learning near the end points of the range, the input and output data were normalized. Second, the learning rate was set at 0.1, and the momentum term was set at 0.3. Afterward the network was initialized with randomly distributed weights and biases when training neural networks in the present study. The network configuration was arrived after watching the performance of different configurations for a fixed number of cycles. Then, learning parameters were changed and learning processes were repeated.

As stated previously, the data set is divided into three subsets including training, verification and test. During the training process, all MLP network models use the same training, verification, and test subsets. To reiterate, the MLP networks are trained by the training subset only. The verification subset is used to check independently on the performance of the networks during training. The deterioration in the verification errors indicates over-learning. If over-learning occurs, the SNN software stops training the network, and restores it to the state with minimum verification error. The verification error is also used by the SNN software to select the appropriate networks. However, if a large number of networks are tested, a random sampling effect can be taken into account, and one may get a network with a good verification error, but this does not guarantee its good generalization. Therefore, a third subset (i.e. the test subset) is used to examine the network's capability of application to new cases and inspect its performance after training.

#### *4.4. Validation of neural network*

Theoretically, the performance of the developed MLP networks is measured in two aspects: one is the root-mean-square error (RMSE) value (Dayhoff 1990), and the other is the coefficient of determination ( $R^2$ ), which can be used as indices to evaluate how well the independent variables considered account for the measured dependent variable and thus test the accuracy of the developed MLP networks. In principle, the lower the RMSE value or the higher the  $R^2$  value is, the better the prediction will be.

Table 5 summarizes all the average RMSE and  $R^2$  values for different MLP networks. It can be seen from Table 5 that the developed MLP network models have good performance in terms of the RMSE and  $R^2$  values except those with one input variable. Although the S/A ratio of test subset is different from training and verification subsets, the RMSE values of the verification and test subsets are reasonably close. Hence it can be concluded that the network is likely to generalize well. Besides, the  $R^2$  values are all greater than 0.90 for the verification and test subsets. These demonstrate a close correlation between the independent variables and the measured dependent variable. In other words, the results indicate the compressive strength of concrete can be fairly accurately estimated using MLP networks.

Table 5 Summary of the RMSE and  $R^2$  values

ANN Model	Root-Mean-Square error (RMSE): MPa			Coefficient of determination ( $R^2$ )		
	Training set	Verification set	Test set	Training set	Verification set	Test set
M3:1-2-1	5.944	5.704	7.927	0.9487	0.9500	0.9015
M3:2-1-1	3.767	4.456	3.315	0.9799	0.9696	0.9708
M3:3-3-1	1.670	2.301	1.678	0.9961	0.9924	0.9919
M3:4-3-1	1.816	2.135	1.599	0.9954	0.9933	0.9922
M3:5-3-1	2.000	1.932	1.739	0.9943	0.9943	0.9915
M3:6-5-1	1.766	2.156	1.677	0.9956	0.9931	0.9907
M3:7-6-1	1.822	1.981	1.681	0.9953	0.9949	0.9921
M4:1-5-5-1	5.975	5.692	8.058	0.9485	0.9500	0.9015
M4:2-2-2-1	3.672	4.621	3.204	0.9807	0.9673	0.9721
M4:3-5-1-1	1.831	2.117	1.774	0.9952	0.9934	0.9896
M4:4-8-5-1	2.019	1.929	1.894	0.9943	0.9944	0.9889
M4:5-13-7-1	1.890	1.809	1.841	0.9949	0.9952	0.9894
M4:6-20-7-1	1.831	1.936	1.713	0.9952	0.9944	0.9908
M4:7-11-10-1	1.706	2.004	1.755	0.9959	0.9939	0.9899

#### 4.5. Neural network analysis results

The main objective of the developed MLP network models in this research is to establish the correlation relationships between pulse velocity and compressive strength of concrete at various ages. Essentially, both  $v$  and  $f'_c$  can be expressed as a nonlinear function of mixture proportions, aggregate type and size, age of concrete, moisture content, and others. Moreover, according to the sensitivity analysis (see Table 4), it is observed that the pulse velocity is the primary variable, which has most influence on the prediction of compressive strength of concrete. Therefore, it seems to be natural to predict concrete strength using pulse velocity. However, if the pulse velocity parameter is used as the sole input variable, such as M3:1-2-1 and M4:1-5-5-1 models, the RMSE value is as high as around 8 MPa for test subset as shown in Table 5.

Table 6 shows the ratio of the measured concrete strength  $f'_{ce}$  to the MLP networks predicted strength  $f'_{cp}$  of each test sample. For M3:1-2-1 model, the average values of these ratios are 0.946, 0.831, 0.818, and 0.754 for concrete with ages at 3, 7, 14, and 28 days, respectively. This indicates that the concrete strength cannot be accurately estimated by using  $v$  as the only input variable. Moreover, the pulse velocities of all the 111 samples given in Table 1 and 2 are adopted to predict the concrete strength using M3:1-2-1 and M4:1-5-5-1 models. The measured concrete strength is plotted against the predicted value as shown in Fig. 4 and the line of equality ( $f'_{ce} / f'_{cp} = 1$ ) is also drawn in the figure. It can be easily observed from Fig. 4 that the distribution of data points are rather scattered. This reveals again that the use of pulse velocity ( $v$ ) as the only input variable cannot have an accurate estimate of concrete strength.

By contrast, the results shown in Table 5 indicate that in addition to  $v$ , inclusion of  $W$  and  $CA$  in the model, such as M3:3-3-1 network, has positive effect upon the accuracy of  $f'_c$  predictions. Besides, using four to seven input variables, the compressive strength  $f'_c$  can be accurately estimated. Figs. 5(a)-5(f) show the comparison between the predicted and measured strength results for various

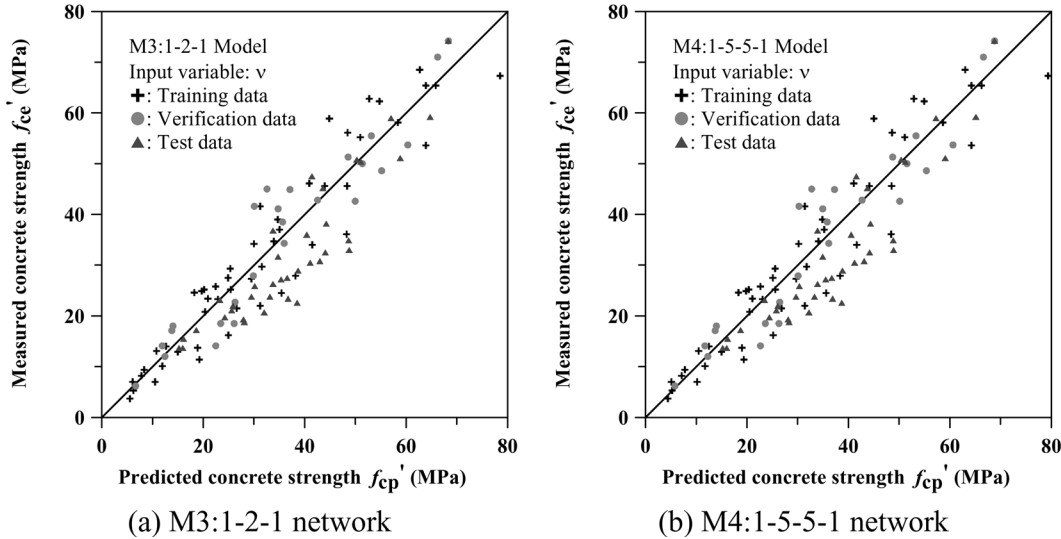


Fig. 4 Measured-versus-predicted strength by ANNs with one input variable

input variables and it clearly shows that the less scatter of data around the line of equality confirms the suitability of these models for prediction of the value of  $f'_c$ .

#### 4.6. Comparison with regression analysis model

There were a lot of expressions proposed by other authors for correlating the concrete compressive strength with the measurements of pulse velocity in the literature. In the study, the ultrasonic pulse velocity in concrete is adopted as independent variable and the compressive strength is the dependent variable. The regression analysis was performed to find the best-fit curves with different functions including exponential and power. In order to compare the neural networks results with those predicted by the regression analysis models, the same 75 records listed in Table 1 (training and verification examples) are used to establish the relationship equations between the pulse velocity and strength of concrete. Figs. 6(a) and (b) show the best-fit curves for exponential and power functions, respectively. The equations obtained from regression analysis are as follows:

- Exponential equation

$$f'_c = 0.0055e^{0.002v} \quad (R^2=0.9147) \tag{11}$$

- Power equation

$$f'_c = 7 \times 10^{-29} \times v^{8.1698} \quad (R^2=0.9116) \tag{12}$$

where  $f'_c$  and  $v$  represent compressive strength (MPa) and pulse velocity (m/sec) of concrete, respectively.

Subsequently, the 36 test data listed in Table 2 used in the neural network models are also adopted to test the accuracy of the regression equations. For comparison purpose, the average  $f'_{ce} / f'_{cp}$  values of the test results for regression models are listed in the last two columns of Table 6. Overall, the developed network models have a much better performance than the regression models in terms of the average  $f'_{ce} / f'_{cp}$  values and the corresponding coefficient of variation (COV). As an example,

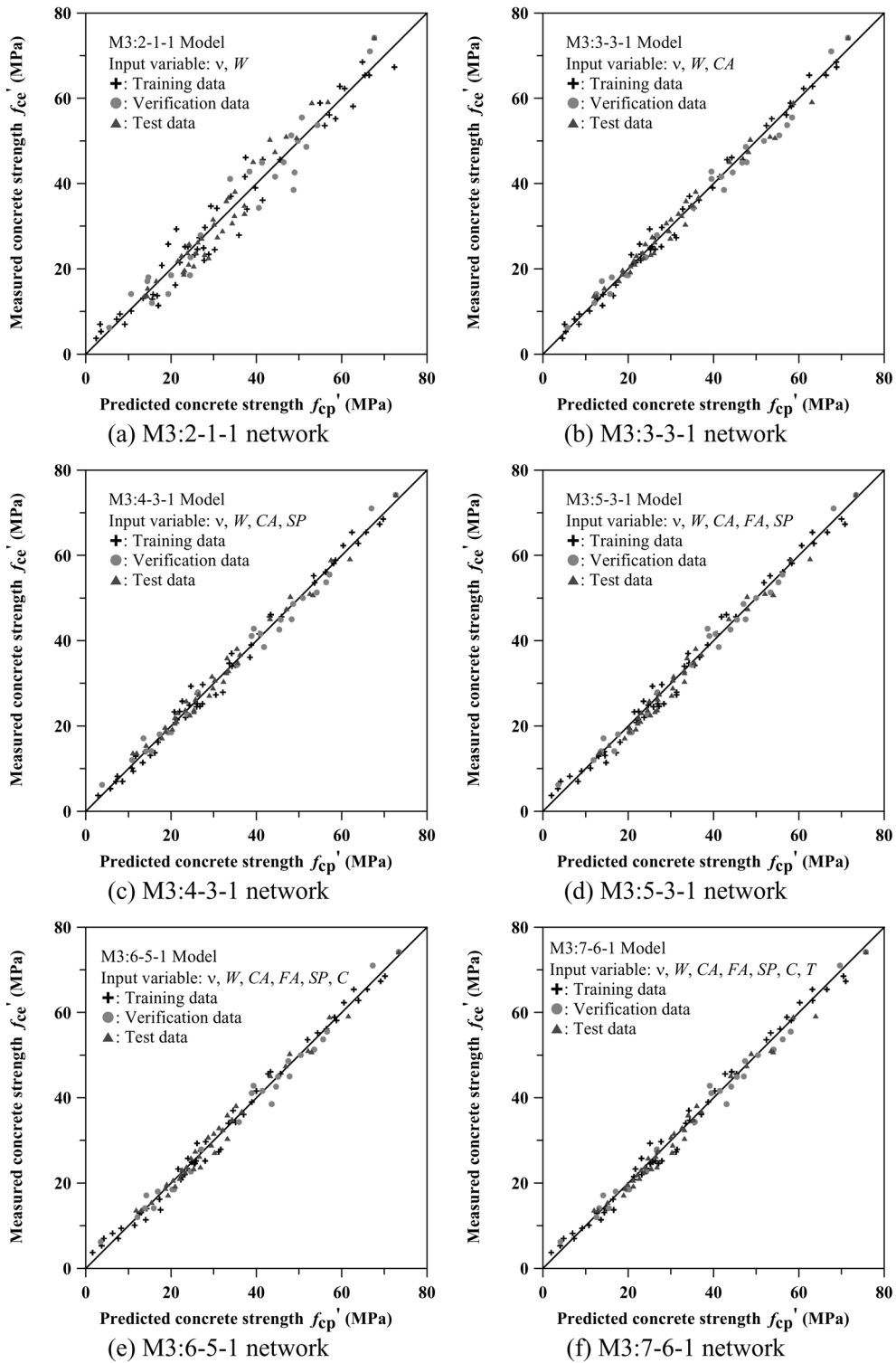


Fig. 5 Measured-versus-predicted strength by ANNs with multi-variable input

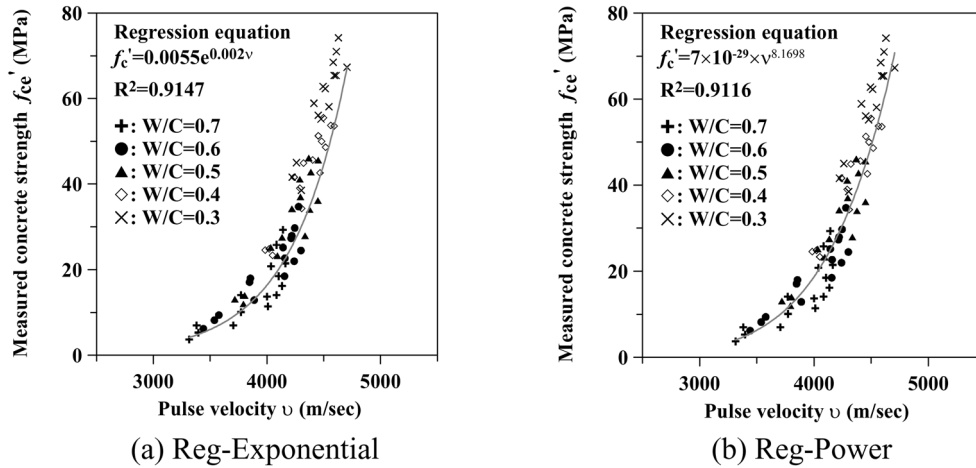


Fig. 6 Correlations between compressive strength and UPV by regression models

for test age of 28 days the average  $f'_{ce} / f'_{cp}$  value and its COV value of M3:7-6-1 model are 0.969 and 4.94%, respectively, while the average  $f'_{ce} / f'_{cp}$  value and its COV value of regression model Reg-E are 0.782 and 14.66%, respectively. Figs. 7(a) and (b) show the data pairs of the measured and the predicted strength values obtained from regression models with exponential and power functions, respectively, and Figs. 7(c) and (d) are the data pairs obtained from the ANN models of M3:3-3-1 and M3:5-3-1, respectively. Figs. 7(a) and (b) show that some data pairs of  $f'_{ce}$  and  $f'_{cp}$  obtained from regression models are located far away from the line of equality as shown in Figs. 7(a) and (b). In contrast with the regression models, the ANN models have much better prediction results and the difference between the predicted and measured strength values is within 10% as shown in Figs. 7(c) and (d). All the results presented in Table 6 and Fig. 7 show that the developed network models are powerful tools for predicting the strength of concrete at different ages.

In this section, the high flexibility of ANN models suitable for analyzing the complicated relationship between the concrete strength and pulse velocity will be demonstrated. Fig. 8(a) shows the distribution of the experimental data pairs of  $f'_c$  and  $v$  (marked as triangular symbols) and those data pairs estimated by the exponential regression model (marked as cross symbols). In Fig. 8(a), the estimated data pairs are distributed along a simple exponential curve conforming to Eq. (11) and this simple curve, however, cannot provide a good prediction due to the scattered distribution of the experimental data pairs. Fig. 8(b) shows the distribution of the experimental data pairs (also marked as triangle symbols) and those data pairs estimated by the ANN M3:3-3-1 model (marked as circular symbols). In Fig. 8(b), the distribution of the estimated data is highly matching with the experimental data pairs. A comparison between Figs. 8(a) and (b) shows that the ANN model is much more flexible than the traditional regression model and very suited for the problem with multiple input variables.

#### 4.7. Computational simulation of strength versus pulse velocity of concrete

Having trained a reliable neural network, one can use it to make predictions on new data. However, a major drawback of ANN application is a lack of its friendliness because neural

Table 6 Measured and predicted concrete strength for test subset

Mix No.	Test age (Day)	Measured compressive strength $f'_{ce}$ (MPa)	Predicted compressive strength $f'_{cp}$ (MPa)							
			ANN model						Regression model	
			M3: 1-2-1	M3: 3-3-1	M3: 4-3-1	M3: 5-3-1	M3: 6-5-1	M3: 7-6-1	Reg-E	Reg-P
N16	3	13.7	16.0	11.9	11.0	13.1	11.8	12.0	15.8	15.9
N17	3	13.7	15.2	12.6	11.9	13.5	13.0	12.9	15.1	15.1
N18	3	15.5	16.1	14.4	14.1	15.5	15.4	15.1	16.0	16.0
N19	3	17.2	18.6	17.9	17.9	19.2	19.3	18.9	18.4	18.5
N20	3	19.7	24.2	18.7	18.6	20.3	19.0	19.8	23.8	23.9
N21	3	21.1	25.6	21.5	21.3	22.8	22.0	22.6	25.0	25.1
N22	3	23.1	23.3	21.9	21.5	23.1	22.6	23.0	22.9	23.0
N23	3	36.8	33.8	36.5	36.2	37.2	36.6	37.2	32.7	32.4
N24	3	47.5	41.4	48.2	47.1	48.0	46.9	47.8	39.9	39.0
Avg. of $f'_{ce}/f'_{cp}$			0.946	1.040	1.067	0.982	1.016	1.005	0.964	0.966
COV of $f'_{ce}/f'_{cp}$			12.20%	5.83%	8.19%	4.69%	7.10%	6.76%	13.01%	13.95%
N16	7	18.8	28.1	18.6	18.7	20.3	18.7	19.2	27.4	27.4
N17	7	19.3	27.9	20.5	20.3	21.8	21.0	21.2	27.2	27.3
N18	7	22.0	25.9	21.3	20.9	22.4	22.2	22.1	25.3	25.4
N19	7	23.8	29.5	26.0	25.4	26.8	26.9	26.8	28.7	28.7
N20	7	27.5	36.6	25.6	26.5	27.3	25.7	26.9	35.3	34.9
N21	7	28.9	38.7	29.6	29.9	30.5	29.5	30.4	37.3	36.7
N22	7	31.7	34.8	30.0	29.6	30.6	30.0	30.7	33.6	33.3
N23	7	45.2	43.6	43.7	43.2	43.6	43.3	44.0	41.9	40.9
N24	7	50.8	50.3	54.4	53.3	54.0	52.9	54.0	48.3	46.5
Avg. of $f'_{ce}/f'_{cp}$			0.831	0.997	1.003	0.961	0.991	0.972	0.858	0.868
COV of $f'_{ce}/f'_{cp}$			15.99%	5.74%	5.06%	6.01%	6.26%	5.37%	16.44%	17.61%
N16	14	20.7	32.0	20.5	20.9	22.2	20.5	21.1	31.1	30.9
N17	14	23.8	33.1	23.4	23.4	24.5	23.6	24.0	32.1	31.9
N18	14	25.9	30.1	24.0	23.6	24.9	24.7	24.7	29.3	29.2
N19	14	27.2	35.4	29.9	29.0	30.2	30.2	30.3	34.2	33.8
N20	14	30.8	43.0	28.9	30.3	30.4	28.7	30.0	41.3	40.3
N21	14	32.5	44.0	32.6	33.0	33.2	32.1	33.2	42.4	41.3
N22	14	36.0	40.4	33.6	33.1	33.8	33.2	34.1	38.9	38.2
N23	14	50.4	51.1	48.6	48.0	47.9	47.8	48.8	49.1	47.2
N24	14	59.0	57.0	58.7	57.5	58.2	57.1	58.7	55.1	52.2
Avg. of $f'_{ce}/f'_{cp}$			0.818	1.021	1.023	0.996	1.025	1.002	0.847	0.867
COV of $f'_{ce}/f'_{cp}$			16.23%	5.05%	4.90%	5.55%	5.31%	4.82%	16.34%	17.78%
N16	28	22.6	38.5	23.6	24.4	25.2	23.3	23.8	37.1	36.5
N17	28	23.4	36.7	25.3	25.4	26.3	25.3	25.4	35.4	35.0
N18	28	26.3	33.8	26.2	25.7	26.9	26.6	26.4	32.7	32.4
N19	28	30.5	41.1	33.4	32.3	33.2	33.2	33.2	39.5	38.7
N20	28	33.0	48.8	31.8	33.4	33.1	31.3	32.6	46.9	45.2
N21	28	34.9	48.7	35.0	35.6	35.4	34.3	35.4	46.8	45.2
N22	28	38.2	44.2	35.8	35.4	35.8	35.2	36.1	42.5	41.4
N23	28	51.1	58.8	53.3	52.6	52.1	52.2	53.5	56.9	53.8
N24	28	59.2	64.7	63.1	61.9	62.6	61.6	64.0	62.9	58.8
Avg. of $f'_{ce}/f'_{cp}$			0.754	0.978	0.976	0.962	0.989	0.969	0.782	0.808
COV of $f'_{ce}/f'_{cp}$			14.87%	5.30%	5.03%	5.78%	5.63%	4.94%	14.66%	16.12%

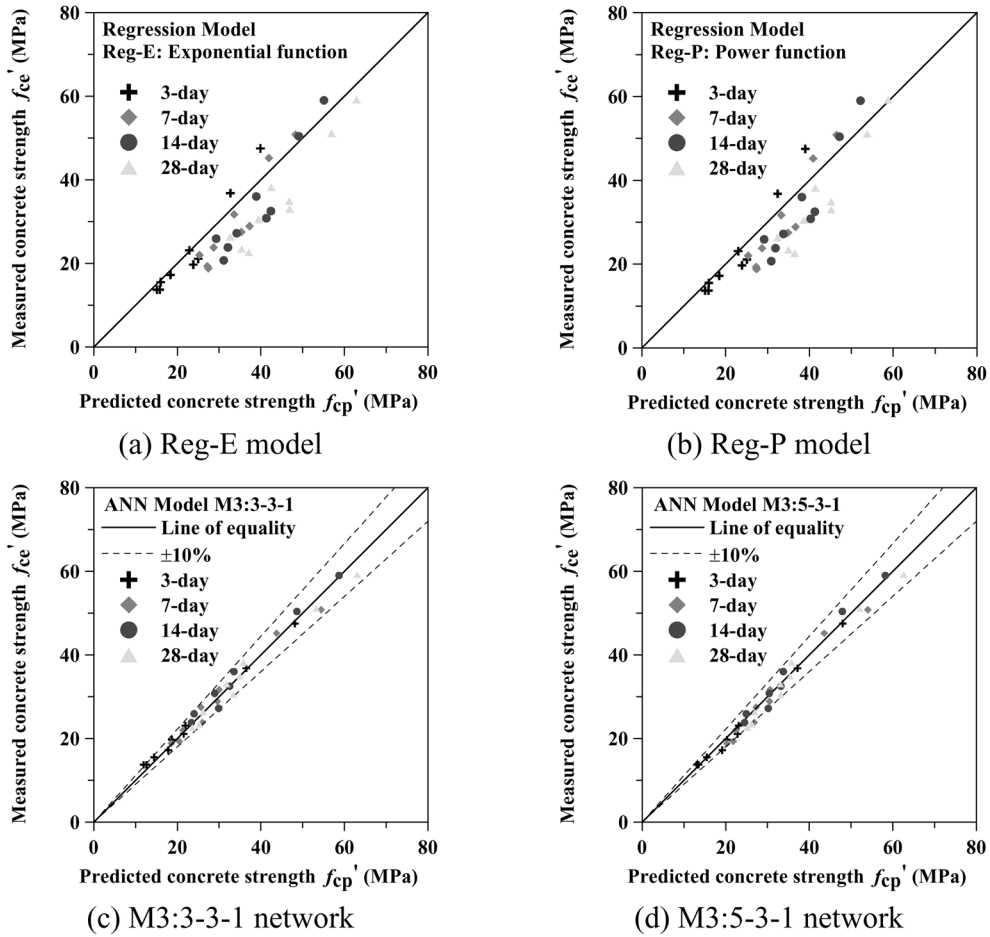


Fig. 7 Comparison between regression analysis and ANN network models

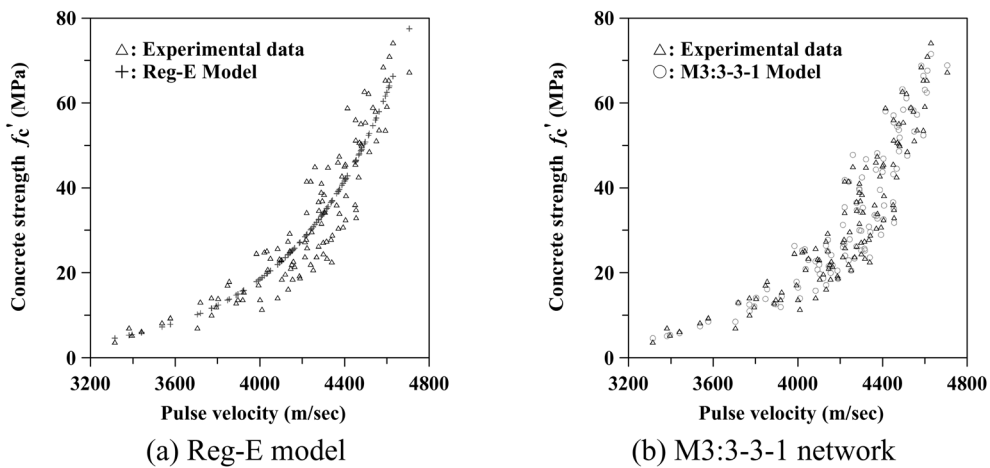


Fig. 8 Plotting of  $f_c'$  versus  $v$

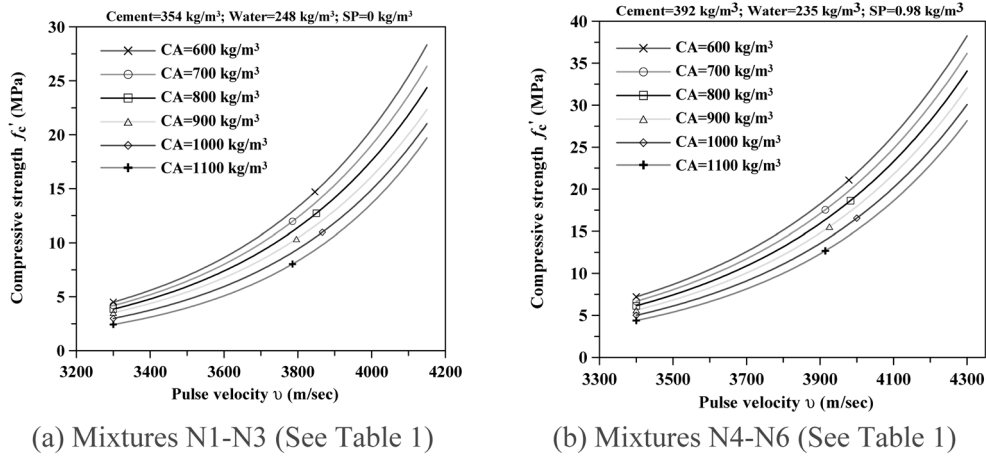


Fig. 9 ANN simulated  $f'_c$  versus  $\nu$  curves of concrete with different mixture proportions

networks do not give explicit knowledge representation in the form of rules, or some other easily interpretable forms. In fact, the trained model is implicit and hidden in the network structure as well as the optimized weights between the nodes. In response to this disadvantage, computational simulation of strength ( $f'_c$ ) versus pulse velocity ( $\nu$ ) of concrete was performed using the trained neural network M3: 7-6-1 model.

The sensitivity analysis of the ANN M3: 7-6-1 model shows that  $CA$  (coarse aggregate content) is the main influential factor of the relationship between  $f'_c$  and  $\nu$  of concrete. Therefore, it is feasible to simulate the  $f'_c$  versus  $\nu$  relationship curves for concrete with a particular  $CA$  value. For example, Fig. 9 shows two ANN simulated charts with six simulation curves of the relationship between  $f'_c$  and  $\nu$  are proposed for concrete with  $CA$  values of 600, 700, 800, 900, 1000, and 1100  $\text{kg/m}^3$ . Also shown at the top of each chart are the cement content, water content, and  $SP$  content of concrete mixture proportions.

To verify the validity of the ANN simulated  $f'_c$  versus  $\nu$  relationship based on  $CA$  in concrete, the measured compressive strengths of specimens having different mixture proportions named from N16 to N22 as listed in Table 2 are compared to those obtained from the ANN charts with the same cement content, water content, and  $SP$  content of concrete mixture proportions. According to the  $CA$  of the specimen, the measured pulse velocity of each specimen can be used to predict its compressive strength by using a linear interpolation between two suitable  $f'_c$  versus  $\nu$  curves. The predicted strengths were compared with the measured values of concrete. Fig. 10 shows the comparison results and all the results are between +10% and -10% of the line of equality. This verifies that the ANN charts for concrete with a particular  $CA$  value can be properly used to predict the compressive strength of concrete with a measured  $\nu$  value. Accordingly, using a well developed ANN model, hundreds of ANN simulated  $f'_c$  versus  $\nu$  curves of various mixture proportions could be established. These ANN charts can serve as a tool to provide a rapid and reliable strength determination for any proposed concrete mixtures with a measured  $\nu$  value.

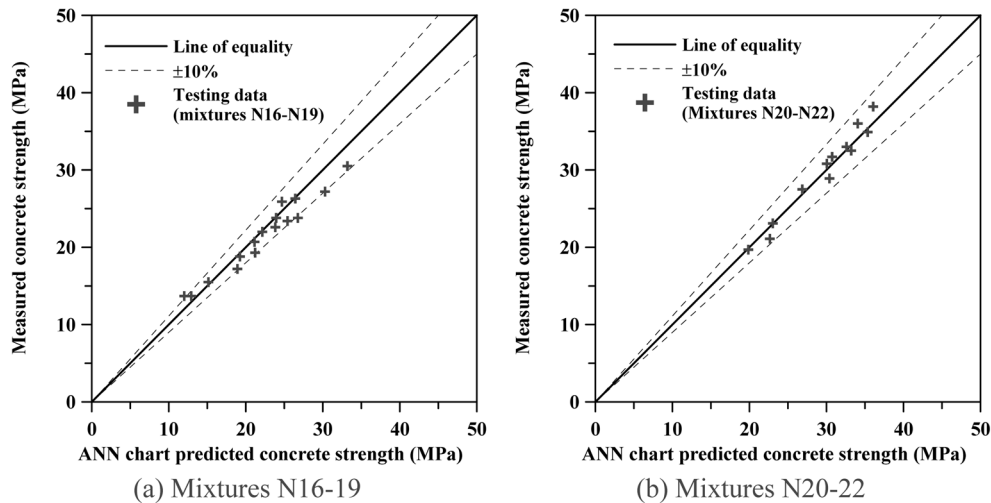


Fig. 10 Comparisons of ANN chart predicted strength with measured strength of concrete

## 5. Conclusions

This paper is focused on establishing a complicated correlation between known input data, such as pulse velocity and mixture proportions of concrete, and a certain output (compressive strength of concrete) using artificial neural networks (ANN). In addition, a comparative study between the neural network and regression analyses has been conducted for establishing the relationships between pulse velocity and strength development of concrete with age. Experimental studies were carried out to evaluate these analytical models.

The results obtained from the studies indicate that the neural networks with three and four layers were successful in learning the relationship between the various input parameters and the single output (compressive strength). The results of the test subset demonstrate that, although the model was not trained for these data, the neural network was capable of generalizing the relationship and yielding reasonably good predictions. Moreover, compared with the conventional approach, the proposed method gives a better prediction both in terms of coefficients of determination and root-mean-square error. It is also shown that the ANN model is much more flexible than the traditional regression model for problems with multiple input variables. On the other hand, computational simulation results verify that the developed ANN charts for concrete with a particular  $CA$  value can be properly used to predict the compressive strength of concrete with a measured pulse velocity. This paper demonstrates that the ANN computational tool is promising to break the long-term constraint encountered in the use of pulse velocity for evaluating the strength of concrete with different mixture proportions.

## References

- Andersen, J. and Nerenst, P. (1952), "Wave velocity in concrete", *J. ACI*, **48**(8), 613-636.
- ASTM C 597-97 (1998), *Standard Test Method for Pulse Velocity through Concrete*, Annual Book of ASTM Standards, Easton, MD, USA.
- ASTM C 39-96 (1998), *Standard Test Method for Compressive Strength of Cylindrical Concrete Specimens*,

- Annual Book of ASTM Standards, Easton, MD, USA.
- Chung, H. W. and Law, K. S. (1983), "Diagnosing in situ concrete by ultrasonic pulse technique", *Concrete Int.*, **13**(10), 42-49.
- Dayhoff, J. (1990), *Neural Networks Architecture*, New York: Van Nostrand Reinhold.
- Demirboga, R., Turkmen I. and Karakoc M. B. (2004), "Relationship between ultrasonic velocity and compressive strength for high-volume mineral-admixed concrete", *Cement Concrete Res.*, **34**(12), 2329-2336.
- Fausset, L. (1994), *Fundamental of Neural Networks*, Prentice-Hall, Englewood Cliffs, N.J., 1994.
- Galan, A. (1967), "Estimate of concrete strength by ultrasonic pulses velocity and damping constant", *ACI J.*, **64**(10), 678-684.
- Ghaboussi, J., Garrett, J. H. and Wu, X. (1991), "Knowledge-based modeling of material behavior with neural networks", *J. Eng. Mech., ASCE*, **117**(1), 129-134.
- Hossain, K. M. A., Lachemi, M. and Easa, S. M. (2006), "Artificial neural network model for the strength prediction of fully restrained RC slabs subjected to membrane action", *Comput. Concrete*, **3**(6), 439-454.
- Jones, R. and Gatfield, E. N. (1955), "Testing concrete by an ultrasonic pulse technique", DSIR Road Research, Tech. Paper No. 34, London, H.M.S.O.
- Kewalramani, M. A. and Gupta, R. (2006), "Concrete compressive strength prediction using ultrasonic pulse velocity through artificial neural networks", *Automation in Construction*, **32**, 374-379.
- Kheder, G. (1998), "Assessment of in situ concrete strength using combined nondestructive testing", *Proceedings of the First international Arab Conference on Maintenance and Rehabilitation of Concrete Structures*, Cairo, 59-75.
- Liang, M. T. and Wu, J. (2002), "Theoretical elucidation on the empirical formulae for the ultrasonic testing method for concrete structures", *Cement Concrete Res.*, **32**(11), 1763-1769.
- Lin, Y., Lai, C. P. and Yen, T. (2003), "Prediction of ultrasonic pulse velocity (UPV) in concrete", *ACI Mater. J.*, **100**(1), 21-28.
- Phoon, K. K., Wee, T. H. and Loi, C. S. (1999), "Development of statistical quality assurance criterion for concrete using ultrasonic pulse velocity method", *ACI Mater. J.*, **96**(5), 568-573.
- Popovics, S., Rose, J. L., John, S. and Popovics, J. S. (1990), "The behavior of ultrasonic pulses in concrete", *Cement Concrete Res.*, **20**(2), 259-270.
- Rumelhart, D. E., Hinton, G. E., and Williams, R. J. (1986), "Learning internal representation by error propagation", *Parallel Distributed Processing*, **1**, 318-362.
- Shikh, M. E. (1998), "Very high strength of special concrete evaluated by pulse velocity", *Proceedings of the 1st international Arab Conference on Maintenance and Rehabilitation of Concrete Structures*, Cairo, 79-105.
- Sturup, V. R., Vecchio, F. J., and Caratin, H. (1984), "Pulse velocity as a measure of concrete compressive strength. In situ/nondestructive testing of concrete", *ACI SP-82*, 01-227.
- Tang, C. W., Chen, H. J., and Yen, T. (2003), "Modeling the confinement efficiency of reinforced concrete columns with rectilinear transverse steel using artificial neural networks", *J. Struct. Eng., ASCE*, June, **129**(6), 775-783.
- Tang, C. W. (2006), "Using radial basis function neural networks to model torsional strength of reinforced concrete beams", *Comput. Concrete*, **3**(5), 335-355.
- Yeh, I. C. (1999), "Design of high-performance concrete mixture using neural networks and nonlinear programming", *J. Comput. in Civil Eng., ASCE*, **13**(1), 36-42.
- Yun, C., Choi, K., Kim, S., and Song, Y. (1988), "Comparative evaluation of nondestructive test methods for in-place strength determination", *Nondestructive Testing*, ACI SP-112, 111-136.
- Zurada, L. (1992), *Introduction to Artificial Neural Systems*, West Publ. Co., USA.
- Zhao, Z. and Ren, L. (2002), "Failure criterion of concrete under triaxial stresses using neural networks", *Computer-Aided Civ. Infrast. Eng.*, **17**(1), 68-73.

## **Notation**

- $C$  = cement content;  
 $CA$  = coarse aggregate;  
 $D$  = depth of the cylinder;  
 $FA$  = fine aggregate;  
 $f'_c$  = concrete compressive strength;  
 $N$  = number of component of the input vector  $X$ ;  
 $O_k$  = calculated output of neuron  $k$ ;  
 $R^2$  = coefficient of determination;  
 $S$  = number of processing elements in the output layer;  
 $SP$  = superplasticizer;  
 $S/A$  = volume ratios of fine aggregate to total aggregate;  
 $T$  = test age;  
 $T_k$  = desired output of neuron  $k$ ;  
 $W$  = Water content;  
 $W/C$  = water-cement ratio;  
 $W_{ji}$  = weighted coefficient between neurons of different layers;  
 $X$  = input vector;  
 $X_i$  =  $i$ th component of input vector  $X$ ;  
 $Y_j$  = network output;  
 $\Delta t$  = measured travel time;  
 $\eta$  = learning rate;  
 $\theta_j$  = bias assigned to neuron  $j$  in the hidden layer;  
 $\theta_k$  = bias assigned to neuron  $k$  in the output layer; and  
 $v$  = pulse velocity

$CC$